JACS
JOURNAL OF THE AMERICAN CHEMICAL SOCIETY

Communication

pubs.acs.org/JACS

Noncovalent Immobilization of a Molecular Iron-Based Electrocatalyst on Carbon Electrodes for Selective, Efficient CO_2-to-CO Conversion in Water

Antoine Maurin and Marc Robert*

Laboratoire d'Electrochimie Moléculaire, Univerity of Paris Diderot, Sorbonne Paris Cité, UMR 7591 CNRS, 15 rue Jean- Antoine de Baïf, F-75205 Paris Cedex 13, France

Supporting Information

ABSTRACT: Catalysis of fuel-producing reactions can be transferred from homogeneous solution to surface via attachment of the molecular catalyst. A pyrene-appended iron triphenyl porphyrin bearing six pendant OH groups on the phenyl rings in all ortho and ortho′ positions was immobilized on carbon nanotubes via noncovalent interactions and further deposited on glassy carbon. X-ray photoelectron spectroscopy and electrochemistry confirm catalyst immobilization. Using the carbon material, highly selective and rapid catalysis of the reduction of CO_2 into CO occurs in water (pH 7.3) with 480 mV overpotential. Catalysis could be sustained for hours without loss of activity and selectivity, and high turnover number was obtained.

In the quest of using CO_2 as a chemical feedstock for producing fuels or precursors to fuels,[1,2] like, e.g., CO that is one reactant in the classical dihydrogen-reductive Fischer−Tropsch chemistry,[3,4] transition-metal complexes have been largely used as catalysts. For example, a number of electrochemically generated low-oxidation states of metal complexes have been proposed for CO_2-to-CO conversion, giving rise to selective and efficient catalysis.[1,5−15] Nonaqueous aprotic solvents have been used for this purpose, mainly acetonitrile or *N*,*N*-dimethylformamide or a mixture of the solvent and weak Brönsted acids (water, alcohols) that have been shown to boost the catalysis.[16,17] However, very few molecular compounds have been able to electrochemically catalyze CO production (a) in pure aqueous conditions and (b) on surface supported conditions, two important requirements from a point of view of practical applications, notably for the design and development of cells associating the cathode compartment with a proton-producing anode by means of a separator. More generally, associating a molecular catalyst to a surface could lead to new, efficient catalytic systems. Regarding CO_2 catalysis in aqueous media, one example concerns the Ni cyclam^{2+},[18−21] although the use of a mercury electrode points to favorable specific interactions of the catalytic species with the mercury surface itself (the recent use of a carbon electrode leads to much less efficiency in terms of rate).[22] A second example involves an electrogenerated tetraphenyl iron(0) porphyrin substituted by trimethylammonio groups at the para position of each phenyl group,[23] leading to selective conversion of CO_2 into CO at pH 7. In order to combine catalytic activity in water with a molecular supported catalyst, one possibility consists of coating the electrode with a film, possibly taking advantage of the catalyst insolubility in an aqueous environment, as it has been done notably with porphyrins and phthalocyanines[24−26] as well as with a Co chlorin complex.[27] In this latter case, CO (80% yield, TON = 1100) was evolved along with H_2 (20% yield) from electrolysis in acidic conditions (pH 4.6) but with large overpotential (700 mV). Another example was recently proposed with a Mn complex cast in a Nafion membrane at pH 7, leading to a TON in CO of 458 and a CO:H_2 ratio of 2:1 with an overpotential close to 750 mV.[28] Very recently, thin films of nanosized metal−organic frameworks incorporating molecular Co porphyrins proved to catalyze the CO_2-to-CO conversion in water with a 76% selectivity and good stability (over 7h) at 700 mV overpotential.[29] Another strategy entails controlled functionalization of surfaces, e.g., by molecular covalent attachment onto carbon surfaces. Examples include the attachment of a Co alkyne-modified porphyrin to an azide-functionalized diamond surface[30] as well as the formation of Co-tpy (tpy = terpyridine) assemblies on glassy carbon electrode after ligand diazotation followed by carefully controlled electrochemical grafting.[31] In the former case, CO_2 catalysis in acetonitrile was proposed to occur at potentials close to −1.35 V vs SHE, but CO formation was only qualitatively assessed via in situ FTIR spectroscopy, while in the latter case, electrolysis at −1.3 V vs SHE in DMF lead to the production of small amount of CO over a 30 min period. Transferring CO_2 catalysis reactivity onto surface thus appears challenging even when using highly active homogeneous catalysts. Moreover none of the two above-described catalysts function in water. Another possibility lies on exploiting noncovalent binding through van der Waals $\pi-\pi$ interactions between a carbon surface and a polyaromatic hydrocarbon, like, e.g., a pyrene unit. A first example was provided by a Re complex bearing two pyrene groups.[32] The modified complex was mixed with carbon black and further deposited on highly oriented pyrolytic graphite. Such a modified electrode proved to be catalytically active in a CO_2 saturated acetonitrile solution, with a CO faradaic yield of 70% and a TON of 58 (1.25 h electrolysis), at a very negative potential of −1.93 V vs SHE, and again not in water as a solvent. Recently an Ir hydride pincer complex modified with a pyrene unit was immobilized onto carbon nanotubes, which were further deposited onto a gas diffusion electrode and finally coated with a polyethylene glycol

Received: December 3, 2015
Published: February 17, 2016

DOI: 10.1021/jacs.5b12652
J. Am. Chem. Soc. 2016, 138, 2492−2495

overlayer.[33] Formic acid was obtained with high yield (83−96%) and TOF (2−7 s^{-1}) during long-term electrolysis (up to 8 h) in CO_2 saturated water, with overpotential larger than 510 mV. This last example is one of the very few where a high catalytic activity was maintained after catalyst immobilization while operating in aqueous conditions. Tetraphenyl iron porphyrins reduced electrochemically to the Fe(0) state proved to be very efficient and selective for the CO_2-to-CO conversion in DMF/phenol and DMF/water mixtures, notably those bearing pendant OH groups in ortho and ortho′ positions on the phenyl rings (e.g., CAT, Scheme 1).[8,34−36] These complexes are however not soluble in

Scheme 1. Iron-Porphyrin Catalysts CAT and CAT_{Pyr}[a]

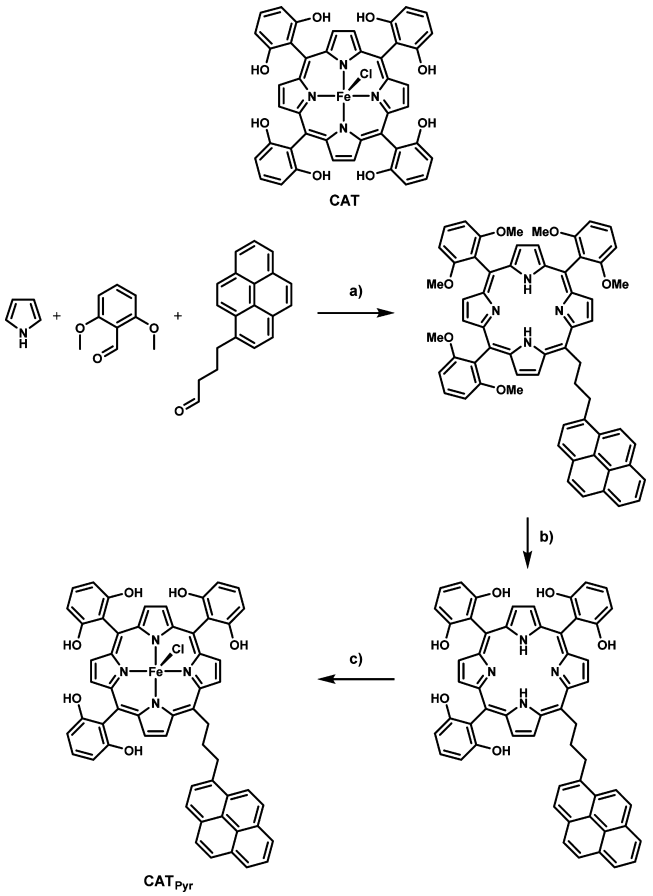

[a]Synthetic procedure for the preparation of CAT_{Pyr}: (a) $BF_3.Et_2O$, $CHCl_3$, then 2,3-dichloro-5,6-dicyanobenzoquinone; (b) BBr_3, CH_2Cl_2; (c) $FeBr_2$, 2,6-lutidine, MeOH.

pure aqueous conditions. By removing one phenyl group and appending a pyrene unit through a short linker (Scheme 1 and Supporting Information), we have prepared a new catalyst, CAT_{Pyr}, that could be immobilized onto carbon surface, while showing high catalytic activity for CO_2 reduction in pH 7.3 water, both in terms of selectivity, durability, and rate.

Cyclic voltammetry of CAT_{Pyr} in DMF at a glassy carbon electrode is shown in Figure 1a. Three distinct monoelectronic reduction waves are observed and respectively assigned to the Fe^{III}/Fe^{II}, Fe^{II}/Fe^{I}, and Fe^{I}/Fe^{0} redox couples. The first two waves are reversible, while the Fe^{I}/Fe^{0} wave is almost reversible with intensity slightly above one electron, due to weak catalysis of residual protons. $E^0(Fe^I/Fe^0) \approx -1.33$ V vs SHE, very close to the value measured with CAT (−1.335 V vs SHE).[36] An intense

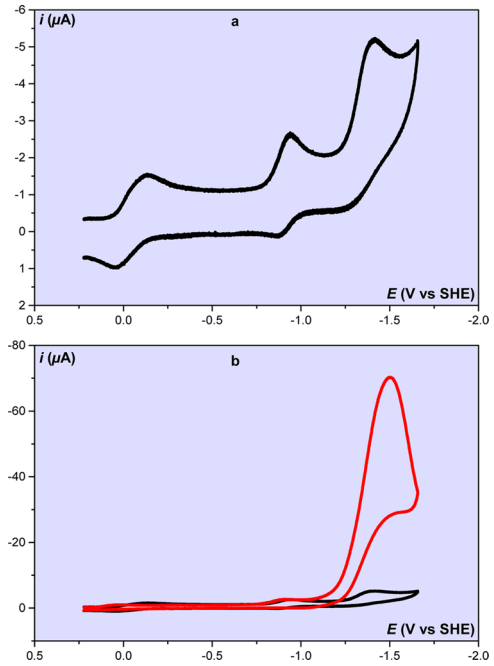

Figure 1. CV (ν = 0.1 V s^{-1}) of CAT_{Pyr} (1 mM) at a glassy carbon electrode (diameter 1.6 mm) in DMF + NBu_4BF_4 0.1 M (a, b) under argon (black trace) and (b) in a CO_2 saturated (0.23 M) solution + PhOH 1 M (red trace).

catalytic peak occurs at the Fe^{I}/Fe^{0} wave in a CO_2 saturated solution in the presence of PhOH 1 M (Figure 1b) as attested by the 50-fold increase of the current. CAT_{Pyr} thus shows similar catalytic activity to CAT in these homogeneous conditions.[34] Encouraged by these preliminary results a suspension of carbon nanotubes (MWCNT, 4 mg·mL^{-1}) in isopropyl alcohol was sonicated for 30 min and deposited onto the glassy carbon surface (see Figure S1 for a SEM image of the modified surface). The electrode was oven-dried, and CAT_{Pyr} (0.2−1 mM) was then deposited on the modified surface (see Figure S1). The material was carefully rinsed with ethanol and finally air-dried. When interrogated by X-ray photoelectron spectroscopy (XPS), unmodified electrodes show only peaks for carbon (C 1s) and nitrogen (N 1s), with a small contribution from oxygen (O 1s) and chlorine (Cl 2p) (Figure 2a and Figure S2). Following

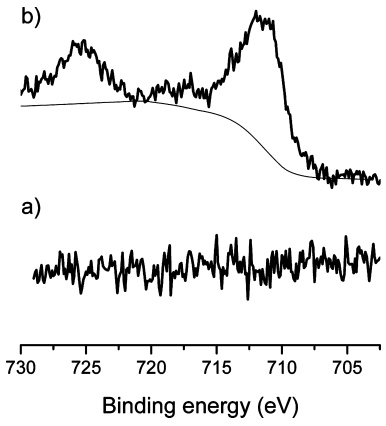

Figure 2. XP spectra in the Fe 2p region for (a) a clean electrode without immobilized iron complex and (b) an electrode with immobilized CAT_{Pyr}. Data show Fe 2p1 and 2p3 peaks at 725.4 and 711.3 eV, consistent with Fe^{III} in CAT_{Pyr}.

DOI: 10.1021/jacs.5b12652
J. Am. Chem. Soc. 2016, 138, 2492−2495

modification with nanotubes and CAT_{Pyr}, new peaks appear that are fully consistent with Fe^{III} (Fe 2p, Figure 2b and Supporting Information (SI)). Nitrogen (N 1s), oxygen (O 1s), and chlorine (Cl 2p) peaks are all enhanced as expected from porphyrin immobilization (Figure S2). Note that carbon peaks exhibit shoulders at high energies (285.2 and 286.3 eV, respectively) corresponding to bonding environment (C−C−C, C−C−H, C−C−OH, and C−C−N) characteristic of the porphryin macrocycle. Cyclic voltammetry (CV) of a modified electrode in a DMF solution is shown in Figure 3a (restricted to Fe^{II}/Fe^{I}

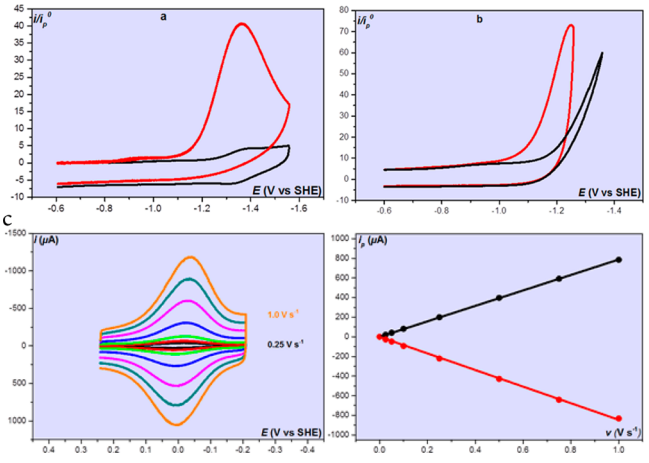

Figure 3. CV (v = 0.1 V s^{-1}) of CAT_{Pyr} ($\Gamma = 7.7 \times 10^{-10}$ mol cm^{-2}) immobilized on MWCNTs deposited onto a glassy carbon electrode (a) in DMF + NBu_4BF_4 0.1 M under argon (black trace) and in a CO_2 saturated solution (0.23 M, red trace); (b) in water + $KHCO_3$ 0.1 M and $KClO_4$ 0.1 M under argon (black trace) and after saturation with CO_2 (red trace); and (c) Fe^{III}/Fe^{II} wave in acidic water (pH 1.4) + $KClO_4$ 0.1 M under argon as a function of the scan rate, at a catalyst concentration of 2×10^{-8} mol cm^{-2}.

and Fe^{I}/Fe^{0} redox couples). It is seen that the Fe^{II}/Fe^{I} redox wave is small under argon atmosphere, due low surface concentration of the porphyrin, while the Fe^{I}/Fe^{0} wave is more intense because of a weak catalysis of residual protons (black trace, Figure 3a). Upon CO_2 saturation, a large increase of the current (by a factor of ∼40) is noticed, showing that the high catalytic activity of the iron complex has been successfully transferred to the heterogenized conditions. Remarkably, the same behavior was found in water (pH 7, Figure 3b), where the modified electrode shows a large increase of the current under a CO_2 atmosphere at potentials negative to −1 V vs NHE. In CV experiments, the amount of electroactive surface catalyst was assessed either by integrating the charge at the level of the Fe^{III}/Fe^{II} wave or by plotting the peak current as a function of the scan rate, giving rise to linear relationship that further assessed the efficient immobilization. An example of the electroactive surface concentration quantification in water is given in Figure 3c and was conducted at pH 1.4 since the Fe^{III}/Fe^{II} redox wave is well-defined in these acidic conditions (at high pHs, several redox peaks appear, see Figure S6 for example). Results obtained by both methods were very similar.

Electroactive surface concentration varies from $\sim 2.5 \times 10^{-8}$ to $\sim 10^{-9}$ mol cm^{-2}, depending on the initial concentration of the porphyrin solution used (between 0.2 and 1 mM) when preparing the carbon surface. At the lowest surface concentration investigated ($\Gamma = 7.7 \times 10^{-10}$ mol cm^{-2}, Figure 3a), successive scans in CO_2 saturated water lead to a decrease of the current intensity when the potential was scanned negatively after the catalytic peak (Figure S3), indicating that the catalyst is partially released from the surface, likely because of charge repulsion between the negative charge borne by the complex and the negatively charged electrode (additionally, partial deactivation of the catalyst may also occur). However, at a higher concentration of catalyst ($\sim 10^{-8}$ mol cm^{-2}), the CVs under CO_2 atmosphere kept stable upon multiple cycling (Figure S4).

Bulk electrolysis was thus performed in aqueous conditions (pH 7.3, $NaHCO_3$ 0.5 M, CO_2 saturated) with a surface immobilized CAT_{Pyr} ($\Gamma = 2.4 \times 10^{-8}$ mol cm^{-2}) mixed with a Nafion solution (see SI for details) and deposited on a carbon plate (S = 2.5 cm^2), at a potential of −1.03 V vs NHE. After 3 h of electrolysis, the total charge passed through the solution was 5.4 C (Figures 4a and S5). Analysis of the headspace above the

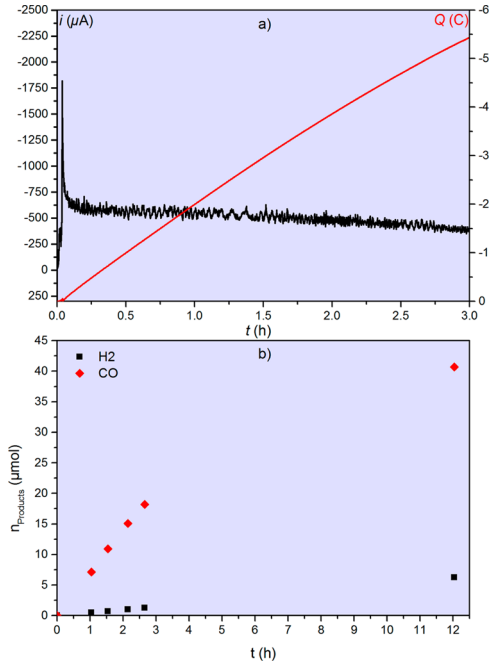

Figure 4. (a) Current (black trace, left) and charge (red trace, right) during bulk electrolysis (E = −1.03 V vs NHE) with CAT_{Pyr} (2.4×10^{-8} mol cm^{-2}) deposited at a carbon surface, in CO_2 saturated water (pH 7.3) + $NaHCO_3$ 0.5 M. (b) The mol number of CO and H_2 produced during the electrolysis.

solution indicates that CO is produced with a very high catalytic selectivity (96:4 CO:H_2 ratio) and an excellent total faradaic yield (97%). During this period, the current remained almost constant, showing the stability of the catalytic system. A TON of 432 in CO (relative to the total quantity of catalyst immobilized onto the cathode) was obtained (TOF 144 h^{-1}). At this pH, a 480 mV overpotential was calculated ($\eta = E^0(CO_2/CO) - (RT/F \times \ln 10 \times pH) - E_{electrolysis} = -0.548 + 1.03$). Blank experiment in an Ar saturated solution gave dihydrogen as a sole product, in low yield. Blank experiment in a CO_2 saturated solution with carbon nanotubes deposited on the carbon electrode also gave H_2 as the only product. Moreover, electrolysis with unmodified physiadsorbed catalyst CAT (Scheme 1) was performed in the same experimental conditions than with CAT_{Pyr}. When identical electroactive surface concentration of the catalyst was used for both cases, a current decrease by a factor 2.2 was observed with CAT (Figure S6), while the faradaic efficiency for CO, although

DOI: 10.1021/jacs.5b12652
J. Am. Chem. Soc. 2016, 138, 2492−2495

good (90%), is also decreased, showing the importance of the attachment mode of the catalyst onto the carbon surface.

The experimental TON may be compared to the theoretical value by using the two following equations:[37]

$$\frac{i}{FS} = \frac{2k[CO_2]\Gamma_{cat}}{1 + \exp\left[\frac{F}{RT}(E - E^0_{cat})\right]} \quad (1)$$

$$\mathrm{TON} = \frac{k[CO_2]}{1 + \exp\left[\frac{F}{RT}(E - E^0_{cat})\right]} \times t \quad (2)$$

where S is the active surface during electrolysis, Γ_{cat} is the catalyst concentration (2.4×10^{-8} mol cm^{-2}), E is the electrolysis potential, E^0_{cat} the catalyst standard potential, k is the first-order rate constant for catalysis, and i the averaged electrolysis current ($Q \times$ faradaic yield$/t/S = 0.186$ mA cm^{-2}). Combining eqs 1 and 2 leads to a TON value of 443, showing that 98% of the catalyst is active within the film deposited onto the surface. Thus, the immobilizing strategy fully maintains the high intrinsic catalytic properties of the porphyrin molecules. The film remains active for a long electrolysis time: after 12 h, a TON value of 813 is obtained (TOF 72 h^{-1}) with a catalytic selectivity of 85% (Figure 4b). The linear variation of the H_2 production with time indicates that the gas evolution is mainly due to the carbon nanotubes, while the catalyst starts being partially deactivated. Optimization of the CAT_{Pyr}/MWCNTs ratio may further increase the performance of the catalytic system.

In conclusion, CAT_{Pyr}, when attached noncovalently to carbon surface, proved to be a selective, stable, and fast catalyst for CO_2-to-CO conversion at low overpotential (480 mV) in neutral pH unbuffered water, outweighing the concurrent water reduction. The iron porphyrin thus joins the short list of molecular catalysts for CO_2 reduction in aqueous media. Finally, the successful transfer of the catalytic activity onto surface opens the way for designing new, highly active catalytic carbon-based materials.

■ ASSOCIATED CONTENT

Supporting Information

The Supporting Information is available free of charge on the ACS Publications website at DOI: 10.1021/jacs.5b12652.

Experimental details and data (PDF)

■ AUTHOR INFORMATION

Corresponding Author

*robert@univ-paris-diderot.fr

Notes

The authors declare no competing financial interest.

■ ACKNOWLEDGMENTS

Fellowship to A.M. from Labex MiChem is gratefully acknowledged. P. Decorse and H. Lecoq (Univ. Paris Diderot) are gratefully thanked for XPS (P.D.) and SEM (H.L.) analysis.

■ REFERENCES

(1) Benson, E. E.; Kubiak, C. P.; Sathrum, A. J.; Smieja, J. M. *Chem. Soc. Rev.* **2009**, *38*, 89.
(2) Aresta, M.; Dibenedetto, A.; Angelini, A. *Chem. Rev.* **2014**, *114*, 1709.
(3) Schwartz, M.; Vercauteren, M. E.; Sammells, A. F. *J. Electrochem. Soc.* **1994**, *141*, 3119.
(4) Dry, M. E. *Catal. Today* **2002**, *71*, 227.
(5) Savéant, J.-M. *Chem. Rev.* **2008**, *108*, 2348.
(6) Rakowski Dubois, M.; Dubois, D. L. *Acc. Chem. Res.* **2009**, *42*, 1974.
(7) Windle, C. D.; Perutz, R. N. *Coord. Chem. Rev.* **2012**, *256*, 2562.
(8) Costentin, C.; Robert, M.; Saveant, J.-M. *Chem. Soc. Rev.* **2013**, *42*, 2423.
(9) Berardi, S.; Drouet, S.; Francas, L.; Gimbert-Surinach, C.; Guttentag, M.; Richmond, C.; Stoll, T.; Llobet, A. *Chem. Soc. Rev.* **2014**, *43*, 7501.
(10) Qiao, J.; Liu, Y.; Hong, F.; Zhang, J. *Chem. Soc. Rev.* **2014**, *43*, 631.
(11) Bourrez, M.; Molton, F.; Chardon-Noblat, S.; Deronzier, A. *Angew. Chem., Int. Ed.* **2011**, *50*, 9903.
(12) Bourrez, M.; Orio, M.; Molton, F.; Vezin, H.; Duboc, C.; Deronzier, A.; Chardon-Noblat, S. *Angew. Chem., Int. Ed.* **2014**, *53*, 240.
(13) Froehlich, J. D.; Kubiak, C. P. *J. Am. Chem. Soc.* **2015**, *137*, 3565.
(14) Smieja, J. M.; Sampson, M. D.; Grice, K. A.; Benson, E. E.; Froehlich, J. D.; Kubiak, C. P. *Inorg. Chem.* **2013**, *52*, 2484.
(15) Mondal, B.; Rana, A.; Sen, P.; Dey, A. *J. Am. Chem. Soc.* **2015**, *137*, 11214.
(16) Bhugun, I.; Lexa, D.; Savéant, J.-M. *J. Am. Chem. Soc.* **1996**, *118*, 1769.
(17) Bhugun, I.; Lexa, D.; Savéant, J.-M. *J. Am. Chem. Soc.* **1994**, *116*, 5015.
(18) Collin, J. P.; Jouaiti, A.; Sauvage, J. P. *Inorg. Chem.* **1988**, *27*, 1986.
(19) Beley, M.; Collin, J.-P.; Ruppert, R.; Sauvage, J.-P. *J. Chem. Soc., Chem. Commun.* **1984**, 1315.
(20) Neri, G.; Walsh, J. J.; Wilson, C.; Reynal, A.; Lim, J. Y. C.; Li, X.; White, A. J. P.; Long, N. J.; Durrant, J. R.; Cowan, A. J. *Phys. Chem. Chem. Phys.* **2015**, *17*, 1562.
(21) Neri, G.; Aldous, I. M.; Walsh, J. J.; Hardwick, L. J.; Cowan, A. J. *Chem. Sci.* **2016**, *7*, 1521.
(22) Froehlich, J. D.; Kubiak, C. P. *Inorg. Chem.* **2012**, *51*, 3932.
(23) Costentin, C.; Robert, M.; Savéant, J.-M.; Tatin, A. *Proc. Natl. Acad. Sci. U. S. A.* **2015**, *112*, 6882.
(24) Furuya, N.; Matsui, K. *J. Electroanal. Chem. Interfacial Electrochem.* **1989**, *271*, 181.
(25) Atoguchi, T.; Aramata, A.; Kazusaka, A.; Enyo, M. *J. Chem. Soc., Chem. Commun.* **1991**, *3*, 153.
(26) Sonoyama, N.; Kirii, M.; Sakata, T. *Electrochem. Commun.* **1999**, *1*, 213.
(27) Aoi, S.; Mase, K.; Ohkubo, K.; Fukuzumi, S. *Chem. Commun.* **2015**, *51*, 10226.
(28) Walsh, J. J.; Neri, G.; Smith, C. L.; Cowan, A. J. *Chem. Commun.* **2014**, *50*, 12698.
(29) Kornienko, N.; Zhao, Y.; Kley, C. S.; Zhu, C.; Kim, D.; Lin, S.; Chang, C. J.; Yaghi, O. M.; Yang, P. *J. Am. Chem. Soc.* **2015**, *137*, 14129.
(30) Yao, S. A.; Ruther, R. E.; Zhang, L.; Franking, R. A.; Hamers, R. J.; Berry, J. F. *J. Am. Chem. Soc.* **2012**, *134*, 15632.
(31) Elgrishi, N.; Griveau, S.; Chambers, M. B.; Bedioui, F.; Fontecave, M. *Chem. Commun.* **2015**, *51*, 2995.
(32) Blakemore, J. D.; Gupta, A.; Warren, J. J.; Brunschwig, B. S.; Gray, H. B. *J. Am. Chem. Soc.* **2013**, *135*, 18288.
(33) Kang, P.; Zhang, S.; Meyer, T. J.; Brookhart, M. *Angew. Chem., Int. Ed.* **2014**, *53*, 8709.
(34) Costentin, C.; Passard, G.; Robert, M.; Savéant, J.-M. *Proc. Natl. Acad. Sci. U. S. A.* **2014**, *111*, 14990.
(35) Costentin, C.; Drouet, S.; Robert, M.; Savéant, J.-M. *Science* **2012**, *338*, 90.
(36) Costentin, C.; Passard, G.; Robert, M.; Savéant, J.-M. *J. Am. Chem. Soc.* **2014**, *136*, 11821.
(37) Costentin, C.; Drouet, S.; Robert, M.; Savéant, J.-M. *J. Am. Chem. Soc.* **2012**, *134*, 11235.

DOI: 10.1021/jacs.5b12652
J. Am. Chem. Soc. 2016, 138, 2492−2495